Coexistence of regularity and irregularity in a nonlinear dynamical system

Kirit S. Yajnik

2/1 Bride Street, Langford Town, Bangalore 560 025, India

A bounded trajectory of a continuous or discrete dynamical system is decomposed into two components. One component, termed as regular, is periodic with a given period and the transformation of the trajectory into the regular component is based on a variational principle. The other component, termed as irregular, is not periodic with the given period. The regular and irregular components have a property similar to orthogonality. The decomposition amounts to representation of the vector space of bounded trajectories as a product of two vector spaces comprising regular and irregular components. The decomposition leads to a new classification of bounded trajectories of a one-dimensional discrete dynamical system into asymptotically regular, mixed and irregular types. It also leads to new measures called periodic mean, periodic covariance and to two measures of irregularity. The potential of these diagnostic tools is explored by detecting windows of period seven, and by elucidating the structure of one such window of the benchmark system governed by logistic map. A window of period k begins with the period-doubling regime having a basic cycle of period k. It is followed by a mixed regime which contains windows of periods of multiples of k. The windows have a similarity property and they are nested.

THERE are many nonlinear phenomena where the behaviour seems regular and easily recognizable as simple in some sense in a certain range of parameters, and is decidedly otherwise in other ranges of parameters. Laminar and turbulent flow regimes of a viscous fluid and periodic and chaotic regimes of nonlinear dynamic systems are classic examples. Thus, one is accustomed to think in terms of the presence or absence of a certain property which lends the air of simplicity or regularity.

Can we think in terms of the behaviour of a nonlinear system as consisting of a regular part and an irregular part? Conventional wisdom seems to suggest that the simultaneous existence of two such opposite characteristics might not be logically permissible. There are, however, instances when one qualitatively thinks of such a possibility. For example, there are several cases of turbulent shear flows, where investigations have revealed a recurring pattern, which is often called a coherent structure. We often describe the observations of the ocean and the atmosphere in terms of a seasonal variation and an anomaly that may be episodic or connected with inter-annual change. What we explore here is a rather general theoretical framework that seeks to open up the possibility of systematic quantitative analysis of the behaviour of nonlinear dynamical systems in such terms.

e-mail: ksy@letterbox.com

Preliminaries

We introduce the basic ideas in a simple way by considering a continuous one-dimensional dynamical system whose state at time t is given by a scalar state variable x. Let $x(t)$ be a trajectory of the system. We will restrict ourselves to bounded trajectories so that $|x(t)|$ is less than some constant C. We seek to represent the trajectory as follows:

$$x(t) = x^r(t) + x^i(t), \tag{1}$$

where $x^r(t)$ satisfies the requirements of regularity, which we will specify in a moment, and $x^i(t)$ does not. Since we wish to make the decomposition unique, we seek a rule that will transform a given trajectory $x(t)$ into its regular component $x^r(t)$.

There is another way to describe our quest. Let us consider continuous and sufficiently differentiable functions on the real line. Let S be the set of bounded functions. We will use continuity but the property of differentiability is not needed for the subsequent development. Any element $x(t)$ of S is a possible trajectory of a one-dimensional dynamical system. To stress the context of dynamical systems, we will call S as the space of all possible bounded trajectories of dynamical systems of one dimension. Note that S is a vector space, if we take addition as point-wise addition, multiplication by a scalar as point-wise multiplication by a scalar, and identity for addition as the trajectory that is zero at all times. Let S^r be the subset of S whose elements meet the requirements of regularity. Then the rule that we seek to transform a given trajectory into its regular component is a mapping of S into S^r.

Now, we would like to choose the requirement of regularity in such a way that S^r is a vector subspace of S.

If we choose periodicity as the requirement of regularity, S^r cannot be a vector subspace as it is not closed under point-wise addition. (The sum of two periodic functions, the ratio of whose periods is irrational, is not periodic.) We choose here periodicity with a given period T as the requirement of regularity. So S^r is closed under addition and scalar multiplication and it is readily seen to be a vector subspace of S.

Let $F[x(t)]$ denote a mapping from S into S^r. Let us consider a few examples.

$$F[x(t)] = \lim_{N\to\infty}\left[\frac{1}{2N+1}\sum_{n=-N}^{N}\{x(t+a+nT)\}^m\right]^{1/m}, \tag{2}$$

where a is a constant and m is an integer. Another example is

$$F[x(t)] = \lim_{N\to\infty}\ln\left[\frac{1}{2N+1}\sum_{n=-N}^{N}\exp\{x(t+a+nT)\}\right]. \tag{3}$$

And yet another one is

$$F[x(t)] = \lim_{N\to\infty}\left[\prod_{n=-N}^{N}x(t+a+nT)\right]^{\frac{1}{2N+1}}. \tag{4}$$

It is not difficult to show that the above rules give trajectories that are periodic with period T. The basic argument is given later for one special case. In view of the available freedom to choose, we need to impose some conditions on the mapping.

Suppose we require that if $x(t)$ is periodic with period T, the mapping should give $x^r(t)$ equal to $x(t)$. That is, such a trajectory should be invariant under the transformation F. This requirement can be met by eq. (2) if a is zero or a multiple of T and m is an odd integer. Equations (3) and (4) can also meet it, if a similar restriction is put on a. We still have a measure of choice.

It is expedient to introduce a binary operation that has some properties of inner product. Let $x(t)$ and $y(t)$ be any two elements of S. Their product $[x(t),y(t)]$ is a scalar given by the following definition.

$$[x(t), y(t)] = \frac{1}{T}\int_0^T \lim_{N\to\infty}\left[\frac{1}{2N+1}\sum_{n=-N}^{N}\{x(t+nT)y(t+nT)\}\right]dt. \tag{5}$$

A variational principle

Now we state our choice in terms of a variational principle. Consider a bounded trajectory $y(t)$ that is periodic with period T and the given trajectory $x(t)$. $[x(t)-y(t), x(t)-y(t)]$ can be interpreted as a global measure of the departure of $y(t)$ from $x(t)$. Consider the periodic trajectory that makes this measure an extremum. That is,

$$\delta[x(t)-y(t), x(t)-y(t)] = 0. \tag{6}$$

Since $y(t)$ is periodic with period T, it then follows that

$$\frac{1}{T}\int_0^T \delta y \lim_{N\to\infty}\left[\frac{2}{2N+1}\sum_{n=-N}^{N}\{x(t+nT)-y(t)\}\right]dt = 0. \tag{7}$$

Since δy is arbitrary, it further follows that

$$y(t) = \lim_{N\to\infty}\frac{1}{2N+1}\sum_{n=-N}^{N}x(t+nT). \tag{8}$$

Therefore, we define the mapping $F[x(t)]$ by the following relation,

$$x^r(t) = F[x(t)] = \lim_{N\to\infty}\frac{1}{2N+1}\sum_{n=-N}^{N}x(t+nT). \tag{9}$$

The above choice is a special case of eq. (2) with a equal to zero and m equal to one. It is easy to verify that the trajectory given by the above rule is indeed periodic.

$$\begin{aligned}
&F[x(t+mT)] - F(x(t)] \\
&= \lim_{N\to\infty}\frac{1}{2N+1}\left[\sum_{n=-N}^{N}\{x(t+(m+n)T)-x(t+nT)\}\right] \\
&= \lim_{N\to\infty}\frac{1}{2N+1}\left[\sum_{n=-N+m}^{N+m}x(t+nT)-\sum_{n=-N}^{N}x(t+nT)\right] \\
&= \lim_{N\to\infty}\frac{1}{2N+1}\left[\sum_{n=N+1}^{N+m}x(t+nT)-\sum_{n=-N}^{-N+m-1}x(t+nT)\right] \\
&= 0,
\end{aligned}$$

as the terms in the last square bracket are bounded.

If we regard the regular component of a trajectory given by the eq. (9) as an approximation having the specified type of regularity, it is optimal in the sense that the global error $[x^i(t), x^i(t)]$ is minimized by it. The irregular component $x^i(t)$ $(=x(t)-x^r(t))$ may then be viewed as local error or a perturbation.

Regularity decomposition and its properties

We now generalize the above formulation to dynamical systems whose state at time t is given by a D-dimensional vector $\mathbf{x}$. Let x_j $(j = 1,2, \ldots, D)$ denote a component of the state variable. Let $\mathbf{x}(t)$ be a bounded trajectory. Let S be the space of possible bounded trajectories of a dynamical system of D dimensions. It is a vector space with addition, scalar multiplication and unity defined in a fashion similar to the earlier case. In

view of previous arguments, we define regular and irregular components for a given period T as follows.

$$(x_j)^r = x_j^r(t) = \lim_{N\to\infty} \frac{1}{2N+1} \sum_{n=-N}^{N} x_j(t+nT), \tag{10}$$

$$(x_j)^i = x_j^i(t) = x_j(t) - x_j^r(t). \tag{11}$$

We have explicitly shown the index j in the above relations only to emphasize that the jth component of the regular and irregular parts of a trajectory depend only on its jth component. The index will not be shown unless it is necessary for clarity or emphasis. The above definitions constitute the regularity decomposition of a bounded trajectory. Analogously, we have for any two bounded trajectories $\mathbf{x}(t)$ and $\mathbf{y}(t)$,

$$(x_j y_k)^r = \lim_{N\to\infty} \frac{1}{2N+1} \sum_{n=-N}^{N} x_j(t+nT) y_k(t+nT), \tag{12}$$

$$(x_j y_k)^i = x_j(t) y_k(t) - (x_j y_k)^r. \tag{13}$$

Now we give basic properties of the regular and irregular components. Their derivation is straightforward and is not given here.

For any $\mathbf{x}(t)$ in S,

$$\begin{bmatrix} (\mathbf{x}^r)^r & (\mathbf{x}^r)^i \\ (\mathbf{x}^i)^r & (\mathbf{x}^i)^i \end{bmatrix} = \begin{bmatrix} \mathbf{x}^r & 0 \\ 0 & \mathbf{x}^i \end{bmatrix}. \tag{14}$$

Consider the set of regular parts of all trajectories in S. We will denote this subset of S by S^r. Then S^r is a vector subspace of S as for any two elements $\mathbf{x}^r(t)$ and $\mathbf{y}^r(t)$ in S^r and for any scalar c,

$$(\mathbf{x} + \mathbf{y})^r = \mathbf{x}^r + \mathbf{y}^r, \tag{15}$$

$$(c\mathbf{x})^r = c\mathbf{x}^r. \tag{16}$$

Similarly, let S^i be the set of irregular parts of all trajectories in S. Then, S^i is also a vector subspace as for any two elements $\mathbf{x}^i(t)$ and $\mathbf{y}^i(t)$ in S^i and for any scalar c,

$$(\mathbf{x} + \mathbf{y})^i = \mathbf{x}^i + \mathbf{y}^i, \tag{17}$$

$$(c\mathbf{x})^i = c\mathbf{x}^i. \tag{18}$$

Since each element $\mathbf{x}(t)$ in S corresponds to the ordered pair $(\mathbf{x}^r(t), \mathbf{x}^i(t))$, S is represented as the Cartesian product $S^r \times S^i$. Furthermore, for any $\mathbf{x}^r(t)$ in S^r and for any $\mathbf{y}^i(t)$ in S^i, with scalar product defined as in eq. (5), $[x_j^r(t), y_k^i(t)]$ is zero. In this sense, these subspaces are orthogonal.

For any two trajectories $\mathbf{x}(t)$ and $\mathbf{y}(t)$ in S,

$$(x_j y_k)^r = x_j^r y_k^r + (x_j^i y_k^i)^r, \tag{19}$$

$$(x_j y_k)^i = x_j^r y_k^i + x_j^i y_k^r + x_j^i y_k^i - (x_j^i x_k^i)^r. \tag{20}$$

If jth component of any trajectory $\mathbf{x}(t)$ in S is periodic with period T, for any trajectory $\mathbf{y}(t)$ in S,

$$(x_j y_k)^r = x_j y_k^r, \tag{21}$$

$$(x_j y_k)^i = x_j y_k^i, \tag{22}$$

$$x_j^r = x_j, \tag{23}$$

$$x_j^i = 0. \tag{24}$$

For any $\mathbf{x}(t)$ in S,

$$((x_j)^2)^r = (x_j^r)^2 + ((x_j^i)^2)^r, \tag{25}$$

$$((x_j)^2)^i = 2x_j^r x_j^i + ((x_j^i)^2)^i. \tag{26}$$

We may call the *regular component* given by eq. (10) as the *periodic mean.* One could call it a phase average, but such a nomenclature appears to be an embellishment as there is no need to introduce a fast variable in the present context. Furthermore, there is likely to be confusion when one wants to deal with two types of regularity, that is, periodicity with two different periods. Finally, we will call $(x_j^i y_k^i)^r$ as the j–kth element of *periodic covariance* matrix of the trajectories $\mathbf{x}(t)$ and $\mathbf{y}(t)$.

Application to a discrete dynamical system

We now elucidate the above ideas by considering their application to a discrete dynamical system. Let $\{\mathbf{x}_m\}$ $(m = 0, 1, 2\ldots)$ be a bounded trajectory of a discrete dynamical system of dimension D. Let the regular component, which we wish to isolate, be periodic with period P. Let $(\mathbf{x}_{pn})$ be the two-dimensional array of P rows and N columns given by

$$(\mathbf{x}_{pn}) = \begin{pmatrix} \mathbf{x}_M & \mathbf{x}_{M+P} & \mathbf{x}_{M+2P} & \bullet & \mathbf{x}_{M+(N-1)P} \\ \mathbf{x}_{M+1} & \mathbf{x}_{M+P+1} & \bullet & \bullet & \bullet \\ \mathbf{x}_{M+2} & \bullet & \bullet & \bullet & \bullet \\ \bullet & \bullet & \bullet & \bullet & \bullet \\ \mathbf{x}_{M+P-1} & \mathbf{x}_{M+2P-1} & \bullet & \bullet & \mathbf{x}_{M+NP-1} \end{pmatrix}, \tag{27}$$

where M is an arbitrary non-negative integer and the indices p and n run from zero to $P-1$ and $N-1$, respectively. As $N \to \infty$, the trajectory gets wrapped into an array of P rows and infinitely many columns, from which the first M terms of the sequence $\{\mathbf{x}_m\}$ are ex-

cluded. Since we are concerned with properties for large m, the exclusion of the first M terms is merely a device to accelerate convergence in numerical simulations. Let the row-wise mean of the array be defined by

$$\mathbf{X}_{pN} = \frac{1}{N}\sum_{n=0}^{N-1} \mathbf{x}_{pn}. \tag{28}$$

The regular and the irregular components, denoted by capital and Greek letters, are then given by

$$(\mathbf{x}_m)^r = \mathbf{X}_m = \mathbf{X}_p = \lim_{N\to\infty} \mathbf{X}_{pN},\ m - M = p(\mathrm{mod}\ P), \tag{29}$$

$$(\mathbf{x}_m)^i = \xi_m = \lim_{N\to\infty} (\mathbf{x}_m - \mathbf{X}_{pN}). \tag{30}$$

It is clear that the regular and irregular components have the properties given earlier. Let x_{jm} and x_{jpn} with a subscript j or k ($j, k = 1, 2,\ldots,D$) denote jth component of the state vector $\mathbf{x}_m$ and jth component of an element of the array $(\mathbf{x}_{pn})$. Row-wise covariance is then given by

$$C_{jkpN} = \frac{1}{N}\sum_{n=0}^{N-1} (x_{jpn} - X_{jpN})(x_{kpn} - X_{kpN}). \tag{31}$$

Then, the periodic covariance is given by

$$((x_{jm})^i(x_{km})^j)^r = C_{jkp} = \lim_{N\to\infty} C_{jkpN},\ m - M = p(\mathrm{mod}\ P). \tag{32}$$

Thus, $\mathbf{X}_{pN}$ and C_{jkpN} are N-term approximations of the periodic mean X_p and the periodic covariance C_{jkp}, and $(\mathbf{X}_{pN} - \mathbf{X}_p)$ and $(C_{jkpN} - C_{jkp})$ are the truncation errors.

We consider now a one-dimensional discrete system. The above notation can then be simplified as the index j takes only one value and the indices j and k can be dropped from the above expressions. Also, the following recursion relations for the one-dimensional discrete system turn out to be useful in numerical simulations.

$$X_{p(N+1)} = X_{pN} + \frac{(x_{pN} - X_{pN})}{N+1}, \tag{33}$$

$$C_{p(N+1)} = C_{pN} - (X_{p(N+1)})^2 + (X_{pN})^2 + \left[\frac{(x_{pN})^2 - (X_{pN})^2 - C_{pN}}{N+1}\right], \tag{34}$$

where X_{p0} and C_{p0} are zero and $N \geq 0$. It is also useful to introduce column-wise averages denoted by $\langle\cdot\rangle$. Clearly,

$$\langle X_{pN}\rangle = \frac{1}{P}\sum_{p=0}^{P-1} X_{pN} = \frac{1}{PN}\sum_{p=0}^{P-1}\sum_{n=0}^{N-1} x_{pn}, \tag{35}$$

$$\langle (X_{pN})^2\rangle + \langle C_{pN}\rangle = \frac{1}{PN}\sum_{p=0}^{P-1}\sum_{n=0}^{N-1} (x_{pn})^2. \tag{36}$$

The terms on the right are array averages and they depend only on the product PN. It then readily follows that

$$\langle X_p\rangle = \lim_{N\to\infty} \frac{1}{PN}\sum_{m=M}^{PN+M-1} x_m = X, \tag{37}$$

$$\langle (X_p)^2\rangle + \langle C_p\rangle = \lim_{N\to\infty} \frac{1}{PN}\sum_{m=M}^{PN+M-1} (x_m)^2 = X^2 + C, \tag{38}$$

where X and C are the periodic mean and the periodic variance of the trajectory when P is one. The preceding equation can be rewritten as

$$\langle (X_p - X)^2\rangle + \langle C_p\rangle = C. \tag{39}$$

The first term on the left side is a non-negative measure of the variation of the regular component over one period. The second term on the left is the column-wise average of the periodic variance of the irregular component and is by definition non-negative. What the above result states is that while the two terms individually depend on the chosen period P, their sum does not. This result is of fundamental importance in the regularity decomposition.

A classification of trajectories

Equation (39) leads us to the following classification of the bounded trajectories of a discrete dynamical system of one dimension.

Case I: $\langle C_p\rangle$ is zero for some P. Let the lowest value of P for which it is zero be $P_{\min}$. Then the regular component for the period $P_{\min}$ is a periodic trajectory to which the given trajectory approaches in the following sense.

$$\lim_{N\to\infty} \frac{1}{N}\sum_{n=0}^{N-1} (x_{M+nP+p} - X_p)^2 = 0, \tag{40}$$

for each $p < P_{\min}$. We call this type of trajectory *asymptotically regular* or of R type.

Case II: $\langle C_p\rangle$ is not zero for any P and varies with P. Consequently, no matter which value of P is selected, the periodic variance cannot be decreased below a certain threshold. This type of trajectory can be termed *asymptotically mixed* trajectory or of M type.

Case III: $\langle C_p \rangle$ is a non-zero constant. In this case, for all values of P and p, X_p is equal to X. This means that the regular component is a constant irrespective of which period P we choose and the periodic variance of the irregular component is a non-zero constant. Such a trajectory can be termed as *asymptotically irregular* or of I type.

It is clear that the attractor set of a trajectory of R type is finite and it has zero dimension. Consequently, a bounded trajectory, whose attractor has a nonintegral dimension, is necessarily of M type or I type.

It should be noted that the notion of regular component has information about the order in which the trajectory visits various points of the phase space, unlike the notion of the attractor or invariant set which do not provide any information about the order. For instance, if two periodic trajectories of period 3 visit three points A, B, and C in order ABC or ACB, they have the same attractor, namely, {A, B, C}.

Logistic map

Now let us consider, as a bench mark example, the system governed by the logistic map, namely,

$$x_{n+1} = ax_n(1 - x_n), \tag{41}$$

where $0 \le x_n \le 1 \le a \le 4$. Let us decompose the trajectory of this system with the given initial condition x_0 and for the given value of the parameter a into regular and irregular components for a given period P. It follows from the properties of the regularity decomposition that

$$(\xi_n^2)^r = X_n(1 - X_n) - \left(\frac{X_{n+1}}{a}\right). \tag{42}$$

The above relation shows that the periodic variance is coupled with the periodic mean due to nonlinearity of the logistic map. When the period P is unity, we have the following simple relation between the periodic variance C and the periodic mean X.

$$C = X(b - X), \tag{43}$$

where b is $(1 - 1/a)$. It further follows that

$$0 \le X \le b;\ 0 \le C \le b^2/4. \tag{44}$$

Hence, b and $b^2/4$ are natural scales for X, C and their N-term approximations.

Numerical results and discussion

Let us now consider a few numerical results. Consider first the case of a equal to 4. The logistic map is well known to be chaotic[1] in this case. Figure 1 shows how the N-term approximation X_{0N} to the periodic mean varies as N increases from 1000 to 100,000 for period $P = 1$

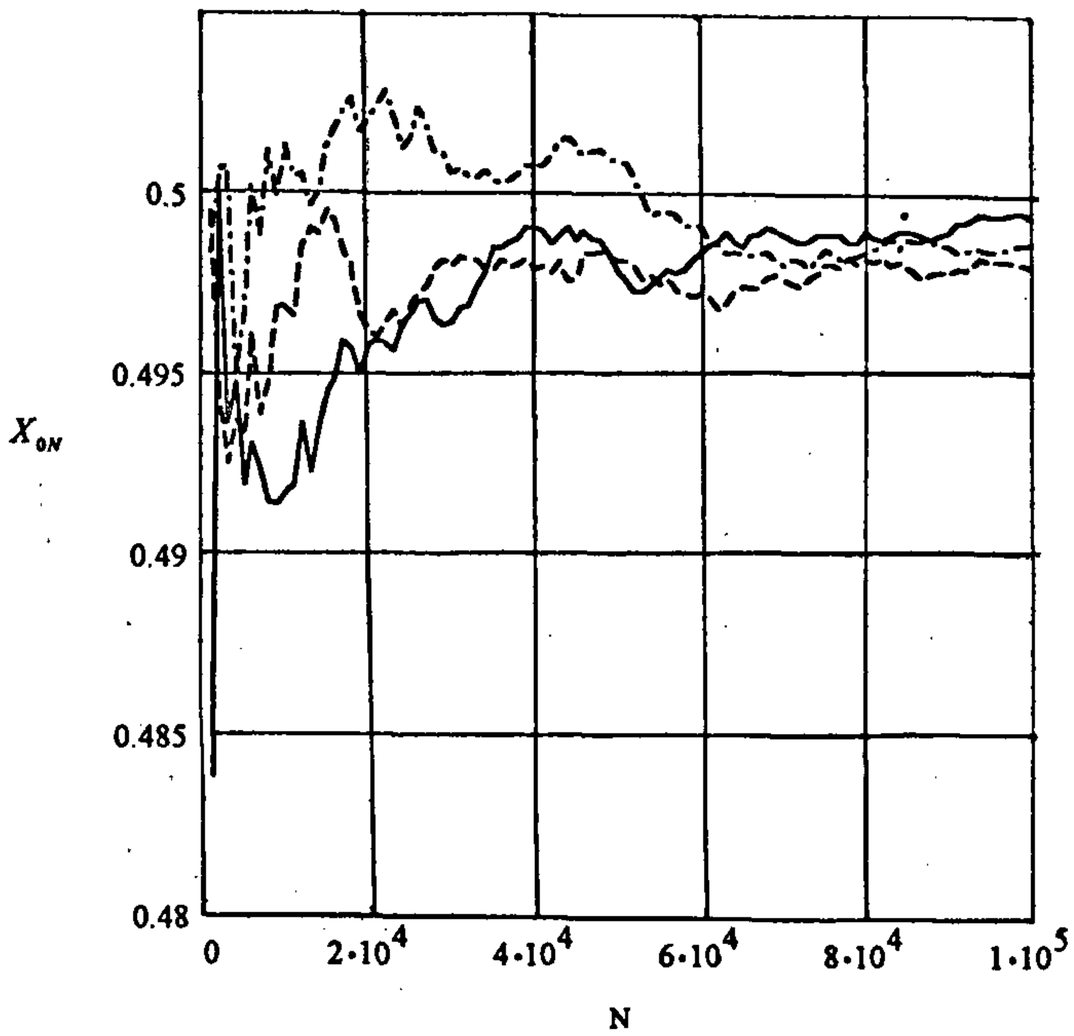

Figure 1. Convergence of the N-term approximation X_{0N} to the periodic mean for the logistic map for three initial conditions. $a = 4$; $P = 1$; $M = 1000$; $\Delta N = 1000$; $x_0 = 0.501$ (----), 0.51(-·-·-), 0.6 (——).

for three initial conditions. There is a clear trend of convergence to a value close to 0.5.

Figure 2 shows the effect of the initial condition on X_{0N} for N equal to 10,000 and 100,000. Clearly, the periodic mean for $P = 1$ for 48 of 51 initial conditions that are scanned is approximately equal to 0.5, the three exceptional initial conditions being zero, 0.25 and 0.5. In these three cases, the trajectory lands on a fixed point (0 or 0.75) and the absence of round-off errors in these exceptional cases enables the numerical simulation to capture trajectories that are unstable.

C_{0N} for P equal to unity behaves similarly and shows a trend towards convergence to 0.125. The effect of initial conditions on C_{0N} is also within the truncation error, except for the three exceptional initial conditions mentioned above.

We now estimate truncation error in the periodic mean for $P = 1$ in a range of the parameter a. The difference $|X_{0N} - X_{0N^*}|$ is shown in Figure 3 for two values of N, namely 1000 and 10,000, with N^* taken as 100,000. Note that the parameter range of [2.8,4] is scanned with a coarse resolution of $\Delta a = 0.01$. The truncation error shows extraordinary variation and is extremely low in a periodic regime away from a bifurcation point. The approach to a bifurcation point is heralded by a rise of about ten orders of magnitude in the truncation error. Detailed examination has revealed that the truncation error away from a bifurcation point decreases like N^{-1} and its low values are due to exponential approach of the trajectory to the asymptotic periodic state. The approach of a trajectory to the asymptotic state at a bifur-

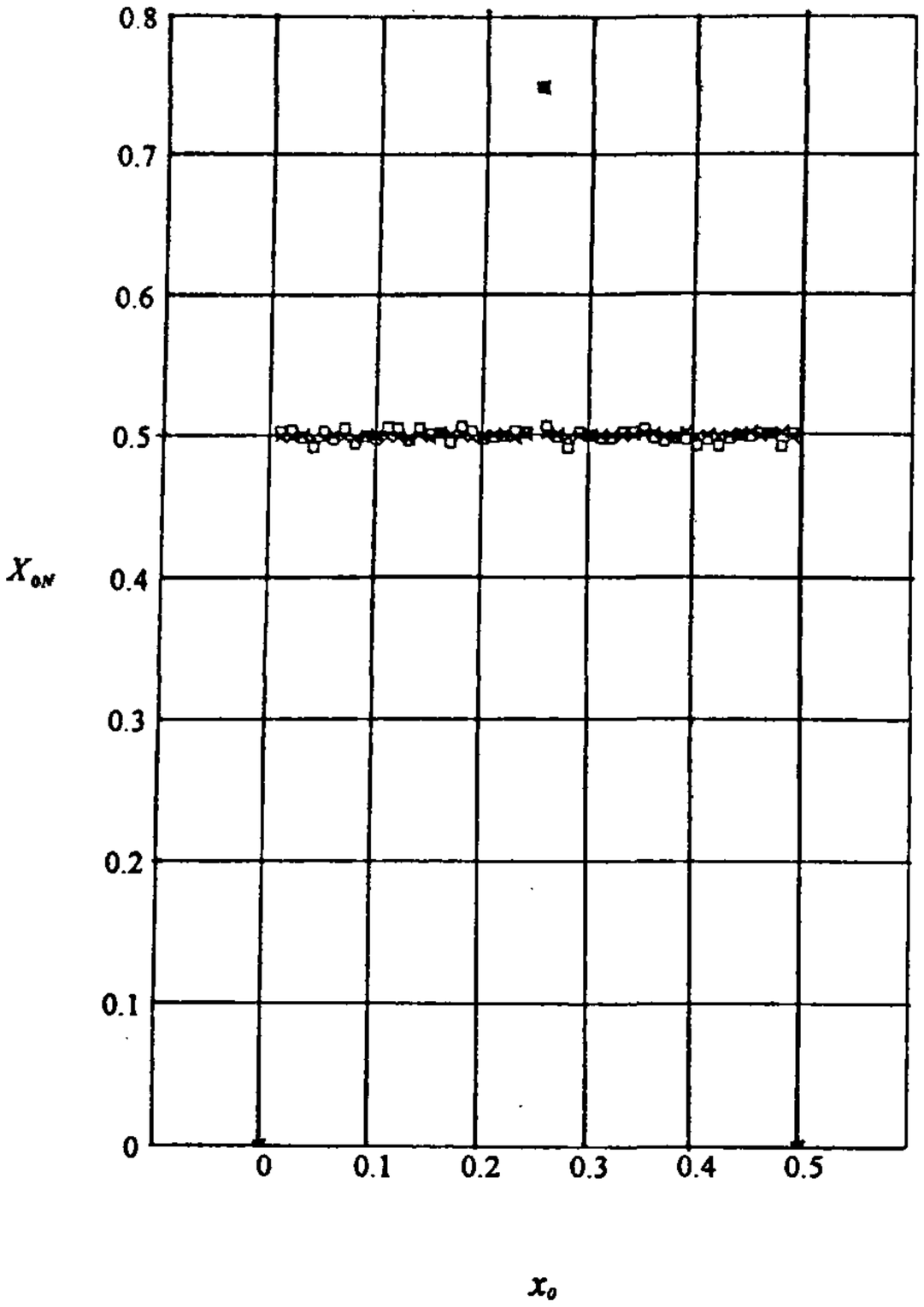

Figure 2. Effect of the initial condition x_0 on the periodic mean for the logistic map. $a = 4$; $P = 1$; $M = 1000$; $x_0 = 0{:}0.5{:}0.01$; $N = 10{,}000$ (□), 100,000 (×).

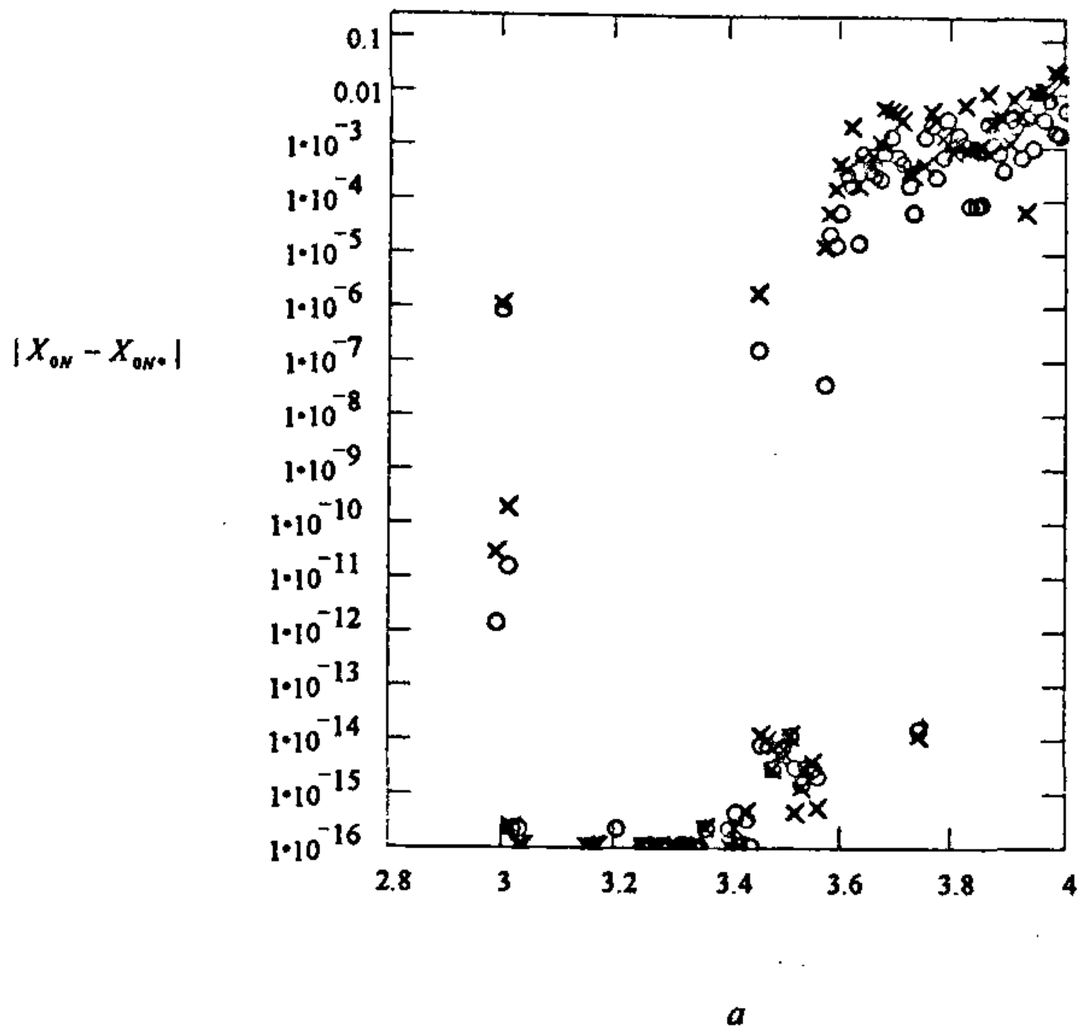

Figure 3. Estimated truncation error in periodic mean in the parameter range [2.8, 4]. $\Delta a = 0.01$; $P = 1$; $M = 1000$; $x_0 = b + 0.001$; $N^* = 100{,}000$; $N = 1000$ (×), 10,000 (○).

cation point is however considerably slower. Figure 4 shows that the trajectory behaviour at $a = 3$ is given by $|x_n - b|/\varepsilon \sim (\varepsilon^2 n)^{-1/2}$ as $\varepsilon^2 n \to \infty$, where $\varepsilon = (x_0 - b)$. The truncation error in the non-periodic regime as shown in Figure 3 is relatively higher but is less than that for a equal to 4.

Extensive computations were carried out for the periodic mean and the periodic variance in the parameter range [3.5, 4] with fine resolution of $\Delta a = 10^{-5}$ for period P varying from 1 to 100 with N equal to 10,000 terms. The initial condition x_0 was taken as 0.1. The first 1000 terms were discarded by setting M equal to 1000.

Let us first consider the case of P equal to one. Figure 5 shows the variation of the periodic mean X_{0N}, which is scaled by b. Similarly, Figure 6 shows the variation of the periodic variance C_{0N}, which is scaled by $b^2/4$. Close connection between the two figures is on account of eq. (43) as shown in Figure 7. Two broad valleys and one wide plateau of X_{0N}/b in Figure 5, which correspond to two wide plateaus and one broad valley in $C_{0N}/(b^2/4)$, are windows for periods 5, 3 and 6. There are numerous other spikes, which are narrow valleys or hills. They are

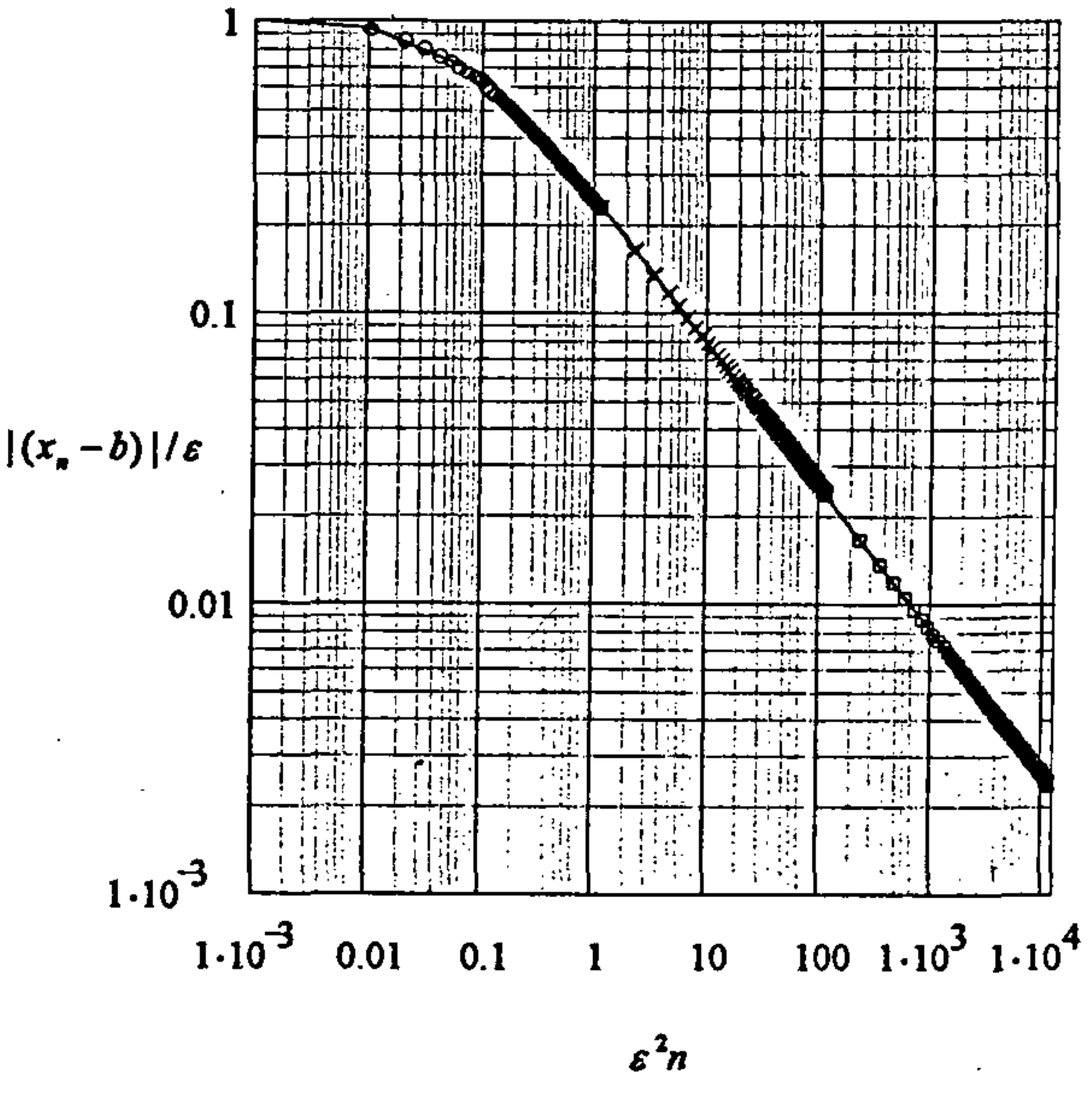

Figure 4. Approach of a trajectory to the asymptotic state at a bifurcation point. $a = 3$; $b = 2/3$; $\Delta n = 1000$; $x_0 = b + \varepsilon$; $\varepsilon = 0.001$ (○), 0.01 (×), 0.1 (□). Interpolation formula (——): $(x_n - b)/\varepsilon = (-1)^n \{\tanh(A(\varepsilon^2 n)^{1/2})\}/(A(\varepsilon^2 n)^{1/2})$; $A = 4.24$.

connected with windows in the fractal/chaotic regime, as we shall see later.

Several reviews and books give excellent accounts of the structure of the period-doubling windows[1–5]. It is sufficient to recall for the present purpose a few proper-

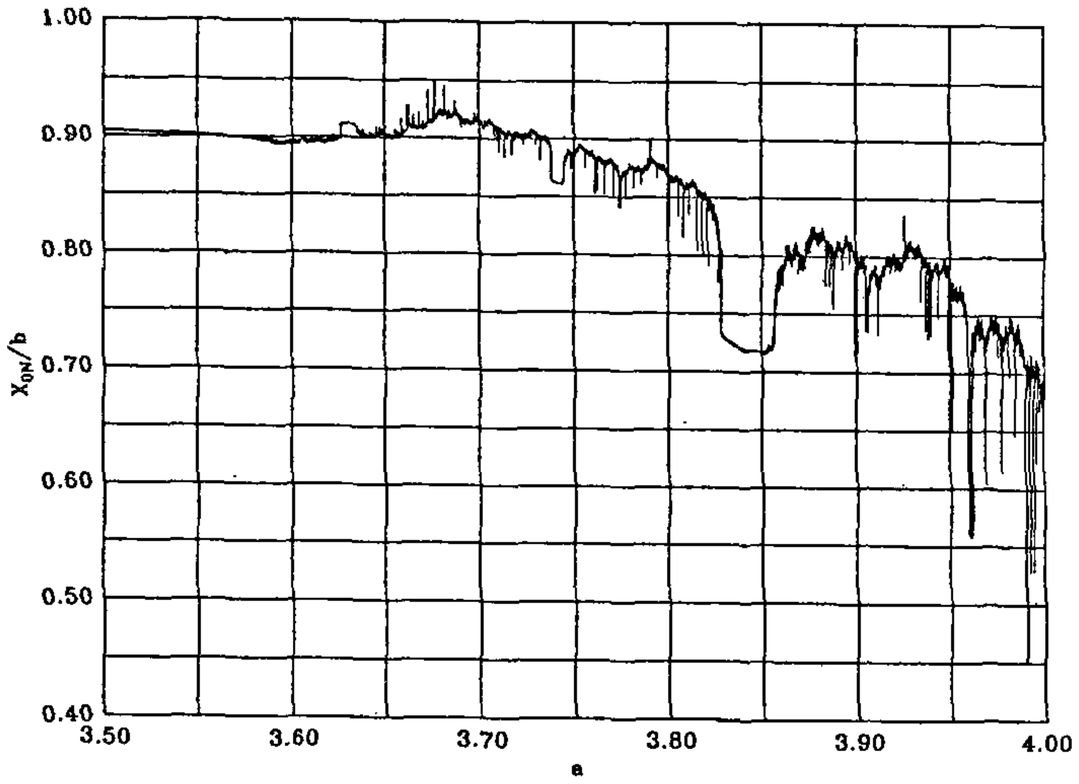

Figure 5. Scaled periodic mean for the logistic map over the parameter range [3.5, 4]. $P = 1$; $\Delta a = 10^{-5}$; $M = 1000$; $x_0 = 0.1$.

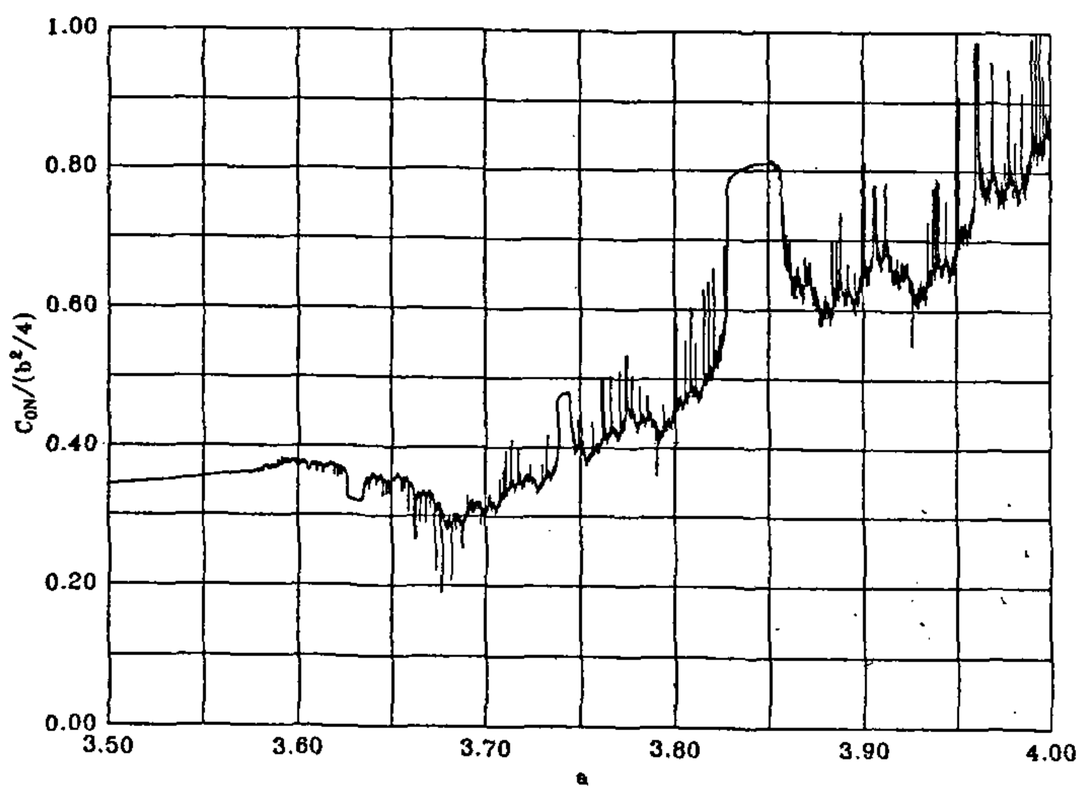

Figure 6. Scaled periodic variance for the logistic map over the parameter range [3.5, 4]. Parameters as in Figure 5.

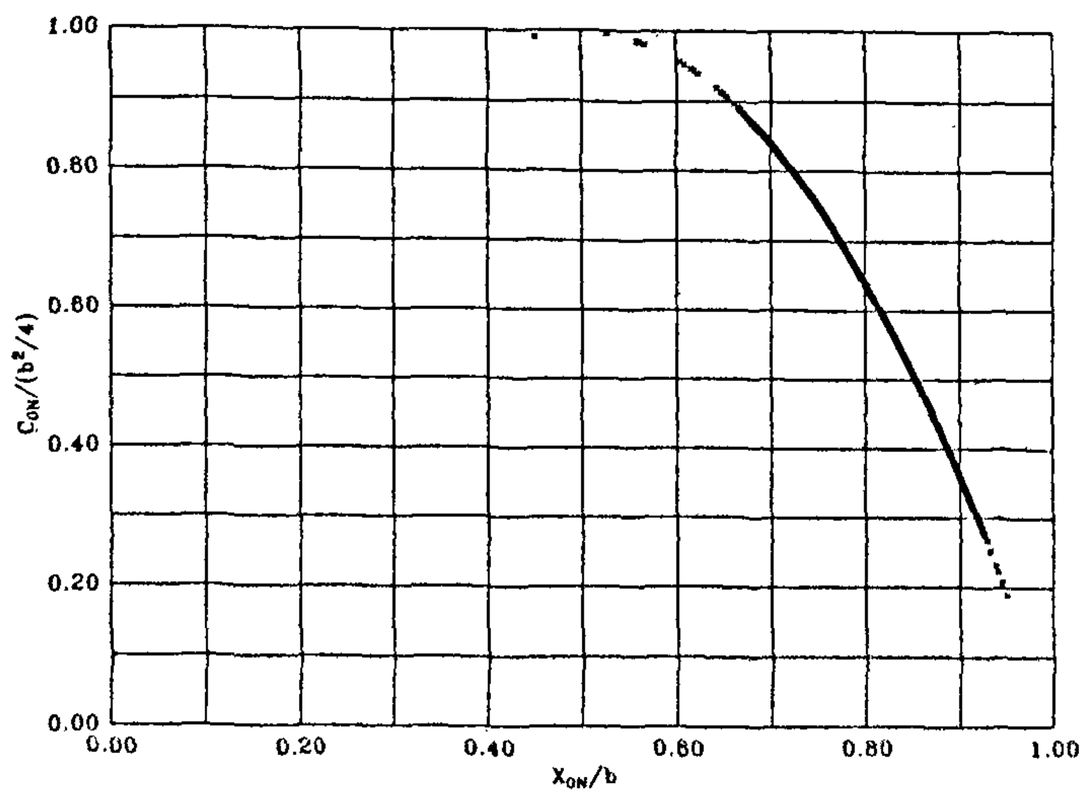

Figure 7. Relationship between scaled periodic mean and scaled periodic variance for the logistic map over the parameter range [3.5, 4]. Parameters as in Figure 5.

ties of the logistic map in the parameter range $1 \le a \le 4$. First, there is at most one stable periodic orbit for each value of a (ref. 1). So there are only two possibilities for any given value of a, that is, either there is one stable periodic orbit or there is none. Second, a period-doubling window of basic period k is a subinterval where the first possibility occurs, and in which there are stable periodic orbits of periodicity $k \cdot 2^n$ with period doubling taking place at pitchfork bifurcations. A window begins with a tangent bifurcation and ends with an accumulation point. Third, although such windows are believed to be dense in the above range, the set of points where the second possibility occurs has non-zero measure[3,6]. The dynamics at such points has exponential sensitivity to initial conditions as manifest by positive Lyaponov exponent. While the dynamics when a is in this set displays some properties of chaos, it is not clear in which subset all the properties required for chaos as given by Devaney hold. For example, when $a > 3.8284$ (ref. 2), there is a cycle with period 3 and as a result of Sarkovskii's theorem[3,7], there are cycles of all periods. This condition implies chaos in the sense of Li and Yorke[8].

It is expedient to introduce two measures of irregularity. (We will exclude from our consideration the region where C is zero, which refers to the case where the trajectory approaches a steady state.) The first measure I_P indicates how large the column average of periodic variance $\langle C_{pN} \rangle$ for a given period P is in comparison with similar quantity C_{0N} for period of unity, both being N-term approximations. The second measure I_{min} indicates the minimum value of I_P when P varies in the range 1 to P_{max}. Thus, the measures are given by the following two definitions.

$$I_P = \langle C_{pN} \rangle / C_{0N}, \tag{45}$$

$$I_{min} = \min_{1 \le P \le P_{max}} (I_P). \tag{46}$$

We will show how the first measure can be used to detect windows of a given period, say, seven. Figure 8 shows how I_7 varies with the parameter a when the interval [3.5, 4] is scanned with the resolution $\Delta a = 10^{-5}$. The first measure is seen to take values close to zero at eight locations, each of which could be an interval or a

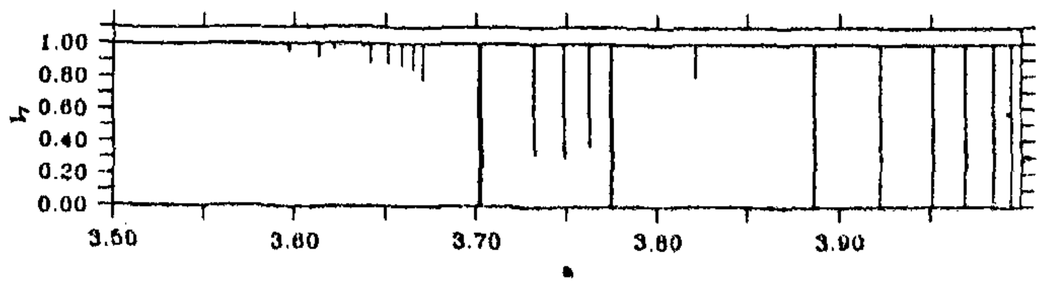

Figure 8. Detection of windows of period 7 by the application of the first measure of irregularity I_7. Δa, M, and x_0 as in Figure 5. Note eight deep valleys where I_7 is close to zero.

Table 1. Windows of period seven detected with resolution $\Delta a = 10^{-5}$

Symbol	Beginning of a cycle of seven, a_1	First bifurcation point, a_2	Beginning of mixed regime, a_3	End of mixed regime, a_4	Window width a_4-a_1
A	3.70166	3.70215	3.70249	3.70279	0.00113
B	3.77414	3.77445	3.77467	3.77485	0.00071
C	3.88604	3.88609	3.88615	3.88618	0.00014
D	3.92219		3.92224	3.92225	0.00006
E	3.95103		3.95106	3.95107	0.00004
F	3.96898			3.96899	0.00002
G	3.98475				
H	3.99454				

point. They correspond to windows of period seven. Their details are given in Table 1. The structure of one such window is discussed in detail later. Combinatorial arguments lead to the conclusion[2] that there are nine period-doubling windows[4] of period 7.

A major qualitative observation is the following. A period-doubling window of basic period k is followed by a mixed regime, where the trajectories that are captured numerically are of M type. In this regime, the periodic variance with period k is small compared to C. The mixed regime also contains periodic sub-windows of period equal to multiples of k. The entire subinterval containing the period-doubling window and the adjacent mixed regime is called in this paper, for brevity, a window of period k. In such a window, $I_k << 1$. Note that by definition, I_1 is unity. Hence k is greater than 1. The first period-doubling window, which is traditionally interpreted as window of period 1, is treated here as window of period 2 for consistency.

The ratio of the window width to resolution Δa is an important parameter for detecting a window as well as for studying its structure. If it is greater than 2, the detection of the window is assured. The ratio has to be much larger for determining detailed structure as will be clear subsequently. It can be seen from Table 1 that as a approaches 4, the window width diminishes rapidly and the resolution of the details of the structure of the window decreases for a fixed Δa.

If the trajectory is asymptotically periodic with a period k less than or equal to P_{max}, I_{min} is very small. Away from a bifurcation point, it is less than about 10^{-20} in double precision computations. So, very low values of $\log(I_{min})$ indicate periodic regimes.

Let us now examine the structure of the first window of period 7. Figure 9 *a* shows that I_7 falls rapidly to zero and remains approximately zero in the window. At the end of the window it rises rapidly. Figure 9 *b* shows X_{0N} for P equal to 1 falls rapidly and remains fairly unaltered throughout the window. It rises rapidly thereafter. Figure 9 *c* shows how $\log(I_7)$ varies in the window A. The graph shows a low flat valley followed by a middle

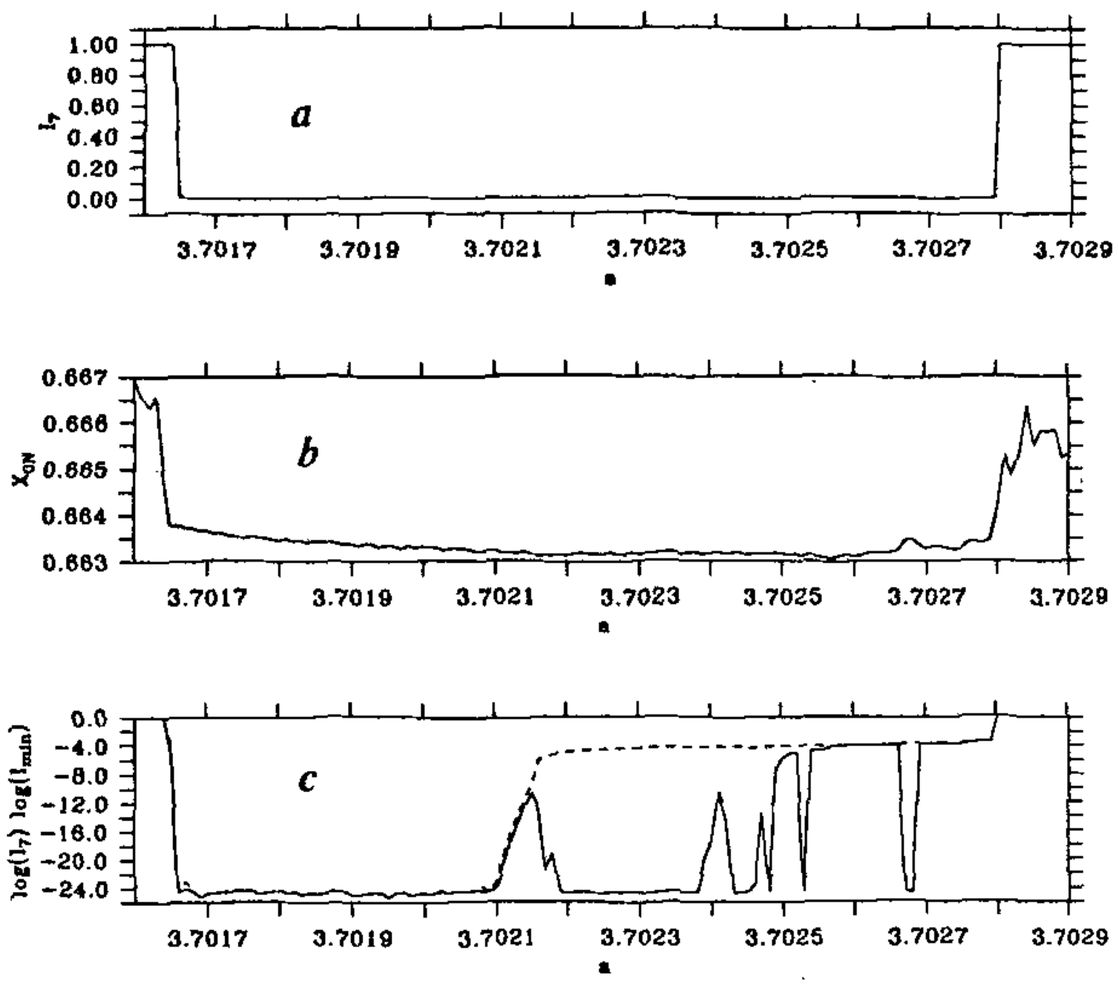

Figure 9 *a–c*. Structure of the window A. Distribution of a, the first measure of irregularity I_7; b, X_{0N} ($P = 1$), and; c, $\log(I_7)$ (---) and $\log(I_{min})$ (——) in the window. The three steep hills in the low-level valley in c indicate bifurcation points and the middle level plateau on the right indicates the mixed regime containing two deep valleys due to periodic windows. Δa, M, and x_0 as in Figure 5.

level plateau. The variation of $\log(I_{min})$ reveals in greater detail the structure of the window. The low flat valley up to the first steep hill corresponds to a periodic regime of period 7. The hills are indicators of bifurcation points. Slow convergence at a bifurcation point leads to a rise in the truncation errors as discussed earlier. The flat valley between the first and the second hill is the periodic regime of period 14. The end of the valley is marked by a sudden rise to a middle level plateau of about –5. The rise portion corresponds to the region near the accumulation point of the period doubling regime containing higher bifurcation points. The middle level plateau has deep valleys of period $7xm$, where m is an integer but not a power of 2.

Figure 10 *a–g* shows how the first measure of irregularity I_P varies with P at several points within and near the window A. Figure 10 *a* shows that it is approximately one for all P in the irregular regime just before the window. Figure 10 *b* shows that this measure has low minima occurring at multiples of 7 at the first point in the deep valley. The graph appears periodic, thus indicating a trajectory of R type with period of 7.

Figure 10 *c* shows minima at multiples of seven at the peak of the first hill. However they differ in two ways from the previous figure. First, the depths of the minima increase slowly. Second, the lowest value of I_P is around 10^{-10}, unlike about 10^{-24} in the previous figure. Both features indicate the effect of truncation errors and the presence of a bifurcation point. Peaks of the steep hills are used to determine the location of bifurcation points. Figure 10 *d* shows a cycle of 14 at the first point after

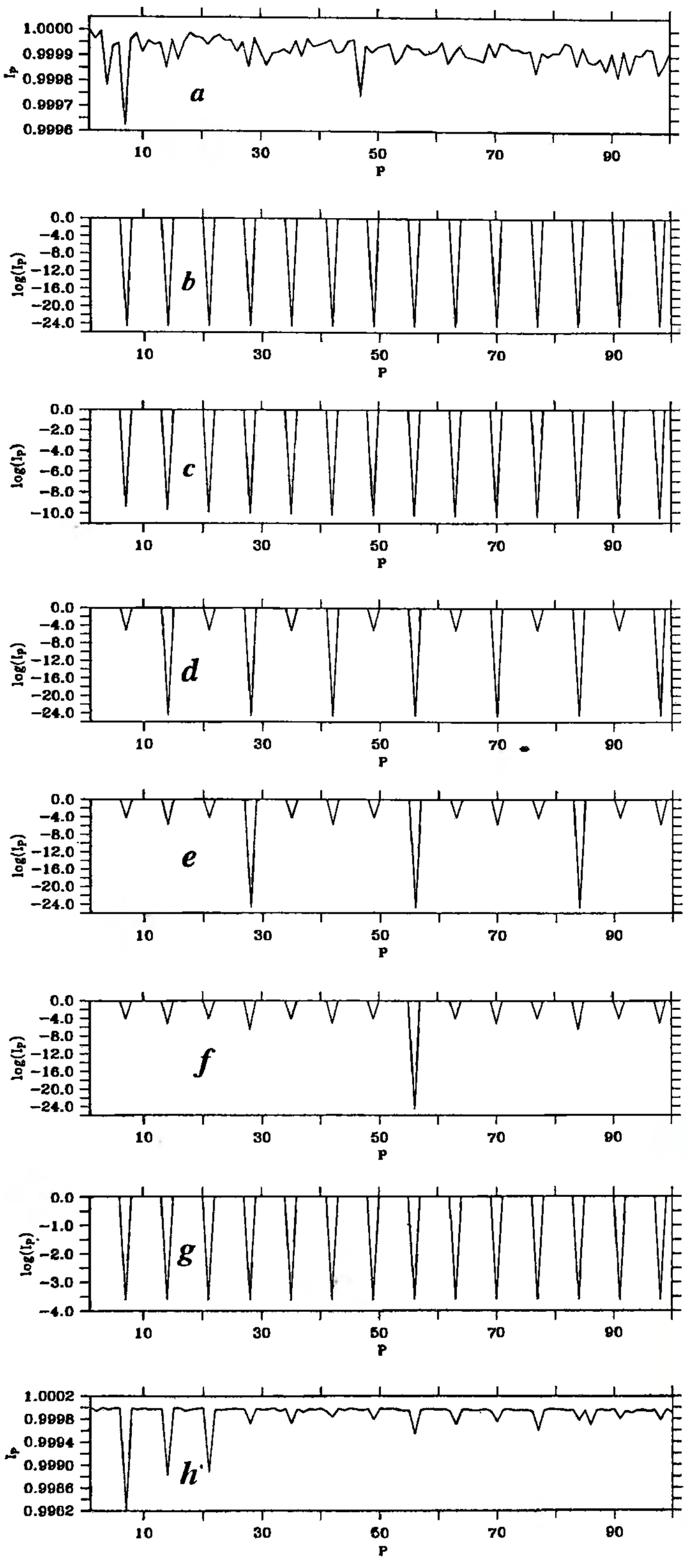

Figure 10 *a–h*. Variation of the first measure of irregularity I_P at several points in and near the window A. *a*, just prior to the beginning of the periodic regime, $a = 3.70163$; *b*, beginning of the cycle of 7. $a = 3.70166$; *c*, first bifurcation point, $a = 3.70215$. (Note the minimas are not as deep as in *b* and there is a slow decrease suggesting truncation error effect); *d*, cycle of 14 after the first peak, $a = 3.70219$; *e*, cycle of 28 after the second peak, $a = 3.70243$; *f*, cycle of 56 after the third peak, $a = 3.70248$; *g*, end of the mixed regime, $a = 3.70279$; *h*, irregular regime after the window. $a = 3.70280$; Δa, M, and x_0 as in Figure 5.

the first hill, thus confirming the presence of the bifurcation point.

The number of bifurcation points that can be determined by this method depends on the value of P_{max}. To detect the nth bifurcation point in the window of basic period k, the period of the cycle after the bifurcation point, namely $k \cdot 2^n$, has to be at most P_{max}. Thus n cannot exceed $\log_2(P_{max}/k)$. Thus, for the basic period of seven, one can detect at most three bifurcation points.

Figure 10 *e* and *f* show the occurrence of cycles of 28 and 56 after the second and the third hill. They are consistent with the interpretation of a hill in the deep valley as a consequence of a bifurcation point in the period doubling regime. Finally, Figure 10 *g* and *h* contrast the behaviour of I_P at the last point in the middle level plateau with the first point in the following high ground. The former shows a periodic character with a period of 7. However, the value of I_P is not sufficiently small to be attributed to truncation errors. On the other hand, I_P is approximately one for all P in the latter case. We conclude that the middle level plateau corresponds to trajectories of M type and the high ground corresponds to the trajectories of I type. The transition from the middle level plateau to the high ground appears to be a bifurcation point, whose nature has yet to be understood.

Figure 11 offers a quick visual way of grasping the qualitative features of a window. It shows for the above window the levels of $\log(I_P)$ for a range of a and P. The changes of periodicity from 7 to 14, subsequently from 14 to 28, at sharp hills are readily noticeable. The contrast between the middle level plateau after the accumulation point and the high ground is also noteworthy.

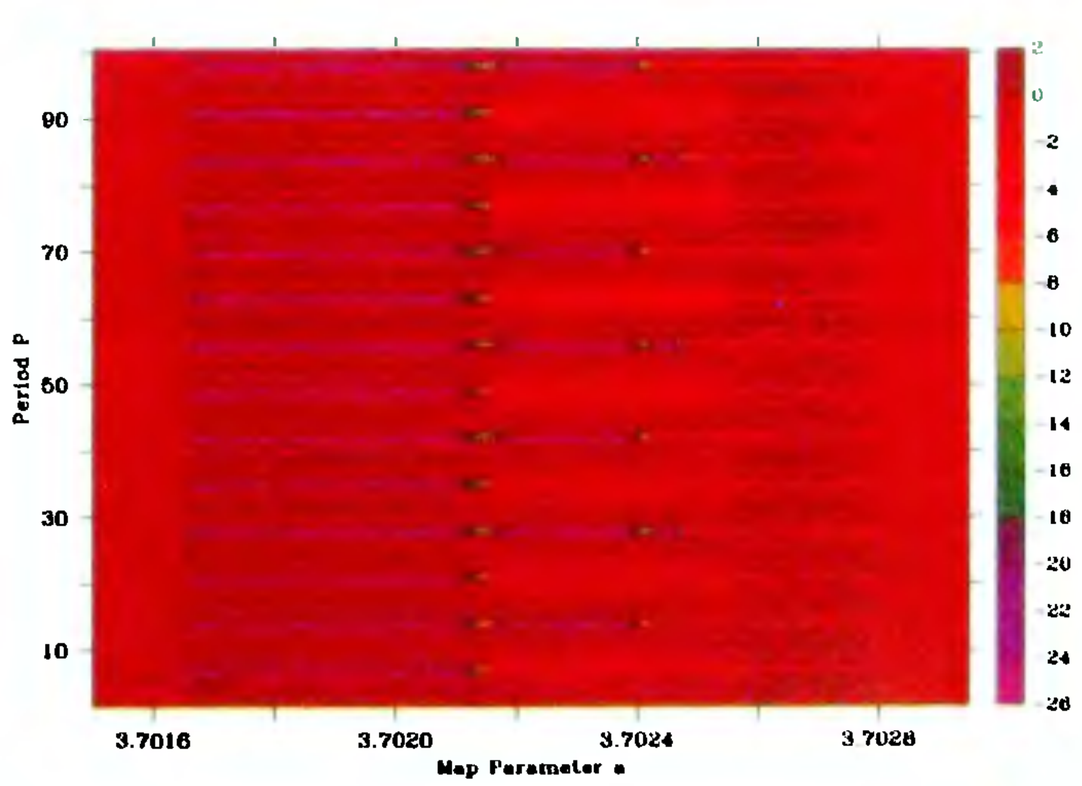

Figure 11. Structure of the first window of period seven is revealed by this Raster plot of the logarithm of the first measure of irregularity. $\text{Log}(I_P)$ is shown to vary with the parameter a and the period P. Horizontal light coloured lines at multiples of 7 on the left indicate the periodic regime of period 7. Transition to period of 14 and 28 is readily noticed. The regime on the extreme right where the colour appears uniform is the irregular regime. One can see the mixed regime between the period-doubling regime and the irregular regime.

Table 2. Structure of the window A

a	X_{0N}	Log I_{min}	Type	Period	Comments
3.70164	0.6654	0.0	*I*		End of irregular regime
3.70166	0.6643	−23.94	*R*	7	Beginning of periodic regime
3.70215	0.6636	−10.56	*R*	7/14	First bifurcation point
3.70241	0.6636	−10.68	*R*	14/28	Second bifurcation point
3.70247	0.6637	−13.42	*R*	28/56	Third bifurcation point
3.70251	0.6637	−5.00	*M*		Beginning of mixed regime
3.70253	0.6636	−24.61	*R*	84	Periodic regime
3.70267	0.6639	−24.63	*R*	21	Periodic regime
3.70268	0.6640	−24.78	*R*	42	Periodic regime
3.70279	0.6639	−3.609	*M*		End of mixed regime
3.70280	0.6646	0.0	*I*		Beginning of irregular regime

Table 3. Salient features of the major windows detected with resolution $\Delta a = 10^{-5}$

Period	Beginning of the basic cycle, a_1	First bifurcation point, a_2	Beginning of mixed regime, a_3	End of mixed regime, a_4	Window width a_4-a_1
2	3.00000	3.44950	3.56990	3.67857	0.67857
3	3.82844	3.84150	3.84944	3.85680	0.02836
4	3.96013	3.96077	3.96120	3.96159	0.00146
5	3.73819	3.74112	3.74301	3.74471	0.00652
5	3.90558	3.90611	3.90646	3.90677	0.00119
5	3.99026	3.99095	3.99033	3.99034	0.00008
6	3.62657	3.63038	3.63272	3.63484	0.00827
6	3.93752	3.93760	3.93765	3.93769	0.00017
6	3.97777	3.97778			

Table 4. Structure parameters of well-resolved windows of periods from 2 to 7

Period	$(a_2-a_1)/(a_4-a_1)$	$(a_3-a_1)/(a_4-a_1)$	$(a_4-a_3)/(a_4-a_1)$
2	0.6624	0.8399	0.1601
3	0.4605	0.7405	0.2595
4	0.4384	0.7329	0.2671
5	0.4494	0.7393	0.2607
5	0.4454	0.7395	0.2605
6	0.4607	0.7437	0.2563
7	0.4336	0.7345	0.2655
7	0.4366	0.7465	0.2535

Table 2 summarizes the main features of the structure identified with the above tools.

The topography of other well-resolved windows is qualitatively similar. Figure 12 *a* and *b* shows the variation of X_{0N}, $\log(I_3)$ and $\log(I_{min})$ for the well-known window of period 3. The low flat valley with steep hills (the period doubling regime) and the middle level plateau (the mixed regime) are much better resolved. In particular, the former shows four out of five possible bifurcation points and the latter shows numerous deep narrow valleys (periodic regimes).

Figure 13 shows the variation of $\log(I_{min})$ over the interval [3.5, 4]. Presence of the middle level plateau is

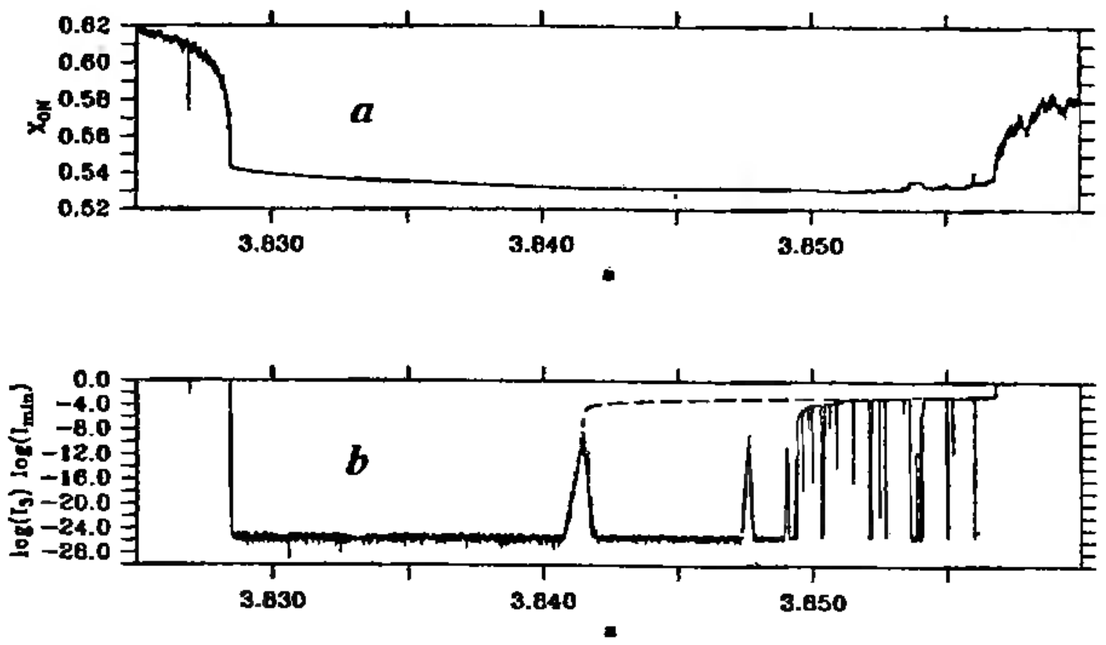

Figure 12. Structure of the window of period 3. The distribution of *a*, X_{0N} ($P = 1$); *b*, first and the second measures of irregularity (I_3 (---) and I_{min} (——)). Note that this window is similar to the window A of period 7, but it is better resolved. Four of the five bifurcation points are indicated by the steep hills in low flat valley on the left in *b*. Also, numerous deep valleys due to periodic windows are seen in the middle level plateau on the right.

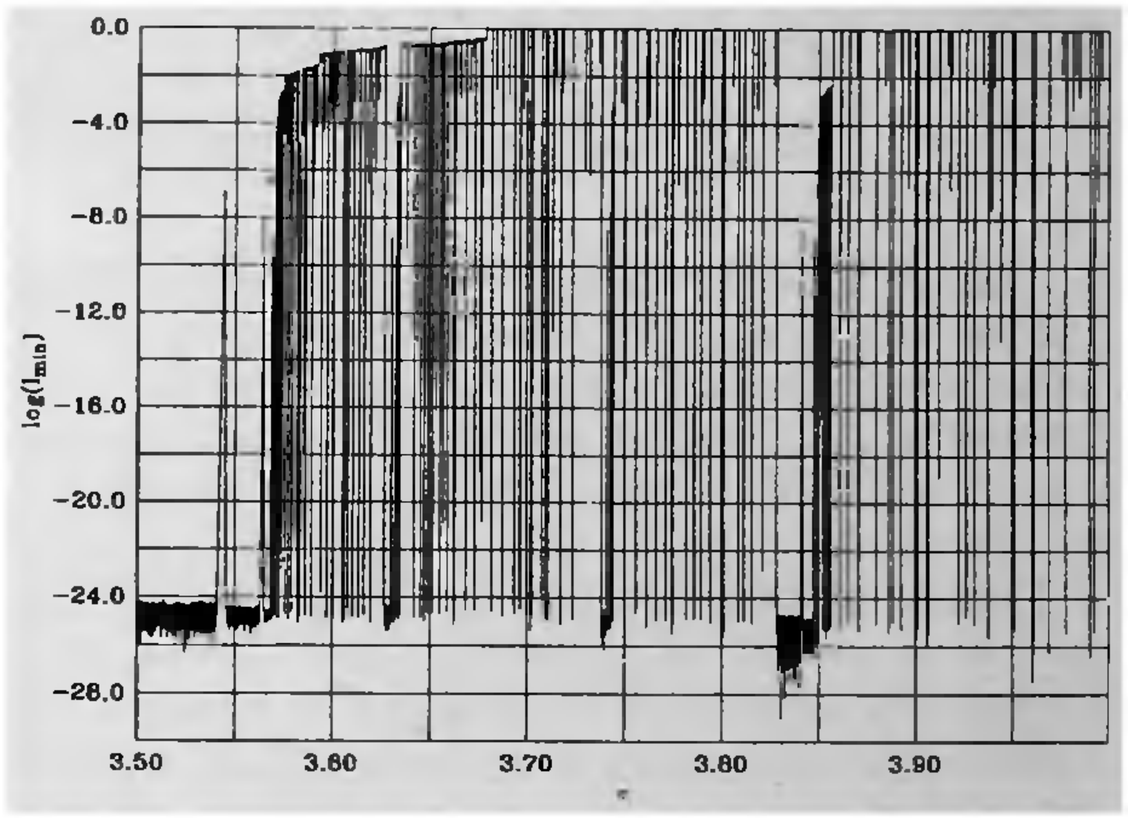

Figure 13. Distribution of the second measure of irregularity in the parameter range [3.5, 4]. Δa, M and x_0 as in Figure 5.

clearly seen in several well-resolved windows, thus confirming that it is a generic feature.

The major features of windows of periods up to 6 observed by the present method are summarized in Table 3. (One window of period 6 is not detected, and the last window given in the table is poorly resolved. Also, the first window is interpreted as the window of period 2 for the sake of consistency as explained earlier.)

The values of a_1, a_2, and a_3 in the above table agree well with the values published in the literature[2] on the beginning of the basic cycle, the first bifurcation point and the accumulation point of these period-doubling windows. A few conclusions can be drawn from the above table. First, the mixed regime occurs only in the range from 3.5699 to 4 and the irregular regime occurs only in the range from 3.67857 to 4. Second, there are

eight well-resolved windows in Tables 1 and 3 where the window width $a_4 - a_1$ exceeds, say, 50 times Δa. If the window width is used for scaling, the resulting structure parameters are given in the Table 4.

The values in the second, third and the fourth column are, respectively, the scaled width of the basic periodic regime, the period-doubling regime and the mixed flow regime. (The values in the last two columns add up to one. Both sets are given here for ease of reference.) One can consider other parameters, which would give the locations of various windows or bifurcation point. If we exclude the first window in Table 4, the structure parameters show little variation. These approximately constant values suggest that the well-resolved windows, with one exception, have a similarity property[9]. One also notices that the mixed regime occurs in roughly one fourth of the window. Finally, the first window of period 6 is nested in the window of period 2. One can see nesting in other windows also (see Figures 12 and 13). Thus, nesting of windows is a generic property.

Concluding remarks

It has been shown that a bounded trajectory of a dynamical system can be decomposed into regular and irregular components. This decomposition leads to a new classification of bounded trajectories of a one-dimensional discrete dynamical system into asymptotically regular (R), mixed (M) and irregular (I) types. It also yields new diagnostic tools like periodic mean, periodic covariance and two measures of irregularity. They have been applied to detect windows of period seven in the dynamical system governed by logistic map and to elucidate the structure of such windows. All the three types of trajectories are found to occur in this system.

Two general implications of the present results are worth noting. First, one can determine numerically the periodic mean and the periodic variance for a given discrete dynamical system for a given P, even when there is exponential sensitivity to initial conditions. These measures are quite robust. In a relatively simple system such as a logistic map, they do not vary with initial conditions except for certain special cases. The special cases correspond to unstable trajectories captured in computations on account of rare absence of round-off errors. Since I_k is very small in a window of period k (> 1), the regular component for period $P = k$ provides a fair approximation to the large time behaviour. The periodic variance gives an estimate of the margin of error. This approximation is optimal in the sense discussed in the paper. So, this is a partial approximate answer to the prediction problem in the presence of exponential sensitivity to initial conditions. Note that in the mixed regime, we end up with a periodic trajectory as an approximation to a non-periodic trajectory. Second, in the inverse problem of determining a map that gives a given bounded trajectory, the periodic mean and the periodic variance for a given value of P determined as above constrain the map.

1. Devaney, R. L., *An Introduction to Chaotic Dynamical Systems*, Benjamin/Cummins, Menlo Park, 1987.
2. May, R. M., *Nature*, 1976, **261**, 459.
3. Ott, E., *Chaos in Dynamical Systems*, Cambridge Univ. Press, 1993.
4. Moon, F. C., *Chaotic and Fractal Dynamics*, John Wiley, New York, 1992.
5. Collet, P. and Eckmann, J.-P., *Iterated Maps on the Interval as Dynamical System*, Birkhäuser, Basel, 1980.
6. Jacobson, M. V., *Commun. Math. Phys.*, 1981, **81**, 39.
7. Sarkovskii, A. N., *Ukr. Mat. Zh.*, 1965, **16**, 61.
8. Li, T. Y. and Yorke, J. A., *Am. Math. Monthly*, 1975, **82**, 985.
9. Yorke, J. A., Greboji, C., Ott, E. and Tedeschini-Lalli, L., *Phys. Rev. Lett.*, 1985, **54**, 1095.

ACKNOWLEDGEMENTS. I thank Dr R. N. Singh, Scientist-in-charge, CSIR Centre for Mathematical Modelling and Computer Simulation (C-MMACS) for use of the facilities at the Centre. I also thank Dr Prabhakar Vaidya for several stimulating discussions during the evolution of these ideas, Dr P. S. Swathi for considerable help in computations and analysis of data using netCDF libraries and Ferret, Steve Emmerson and Russ Dew at Unidata for providing netCDF libraries and Jim Davison at PMEL for providing Ferret. Thanks are also due to M. K. Sharada and R. P. Thangavelu for helpful suggestions. Finally, I wish to thank Prof. Varadachariar Kannan for excellent lectures on chaos, which enhanced my understanding of certain aspects of chaos and indirectly contributed to the manuscript.

Received 1 July 1998; revised accepted 19 June 1999